Acta Metallurgica, Vol. 26, pp. 391–404. Pergamon Press, 1978. Printed in Great Britain

GRAIN BOUNDARY DRAG IN ALLOYS

C. G. SHIRLEY†

Center for the Joining of Materials, Carnegie–Mellon University, Pittsburgh, PA 15213, U.S.A.

(*Received* 2 *August* 1976; *in revised form* 22 *July* 1977)

Abstract—The extrinsic component of the drag force on a grain boundary in an alloy of arbitrary composition and appreciable atomic size disparity is studied in a model in which the boundary is simulated by an externally imposed two-dimensional distortion field. Extrinsic boundary properties arise from processes occurring near, but not in the boundary, so the present study may also be viewed as a study of the coupled concentration and strain fields near a boundary. The results of this paper may be interpreted qualitatively in terms of a velocity and temperature dependent solute–boundary interaction potential. In the limit of small concentrations, this potential becomes velocity and temperature independent so we recover essentially the grain boundary drag theory of Cahn and Lücke and Stüwe. We find that for temperatures close to the coherent spinodal, the grain boundary mobility decreases rapidly with increasing velocity at low velocity, and that this behavior corresponds to a composition profile which is very sensitive to velocity. These effects are less pronounced at higher temperatures. The results apply to velocities less than the breakaway velocity, but the way to extend the theory to higher velocities is indicated.

Résumé—On étudie la composante extrinsèque de la force de traînage sur un joint de grains dans un alliage de composition quelconque oú les constituants présentent des tailles atomiques nettement différentes, à l'aide d'un modèle dans lequel on simule un joint en imposant de l'extérieur un champ bidimensionnel de distorsions. Les propriétés extrinsèques du joint proviennent des processes qui se produisent près du joint, mais pas dans le joint, de sorte que l'on peut interpréter ce travail comme l'étude des champs couplés de concentration et de déformation au voisinage d'un joint. On peut interpréter qualitativement nos résultats en considérant un potentiel d'interaction soluté–joint dépendant de la vitesse et de la température. Dans la limite des faibles concentrations, ce potentiel devient indépendant de la vitesse et de la température, si bien que l'on retrouve essentiellement les résultats de la théorie du traînage des joints de grains de Cahn et de Lücke et Stüwe. Pour les températures proches de la spinodale cohérente, la mobilité du joint de grains diminue rapidement quand la vitesse augmente, aux faibles vitesses; ce comportement correspond à un profile de composition très sensible à la vitesse. Ces effets sont moins prononcés à haute température. Nos résultats s'appliquent pour des vitesses inférieures à la vitesse de libération, mais on indique comment on pourrait étendre la théorie à de plus grandes vitesses.

Zusammenfassung—Es wird die extrinsische Komponente der Reibungsspannung auf eine Korngrenze in einer beliebig zusammengesetzten Legierung mit beträchtlichem Unterschied in den Atomgrößen in einem Modell untersucht, in welchem die Korngrenze durch ein außen angelegtes zweidimensionales Verzerrungsfeld simuliert wird. Die extrinsischen Eigenschaften der Korngrenze rühren von Prozessen nahe, aber nicht innerhalb de Korngrenze her; die vorliegende Untersuchung Kann also als eine Untersuchung der verkoppelten Konzentrations- und Verzerrungsfelder in der Nähe einer Korngrenze angesehen werden. Die Ergebnisse dieser Arbeit lassen sich qualitative mit einem geschwindigkeits– und temperaturabhängigen Wechselwirkungspotential Legierungsstoff–Korngrenze interpretieren. In der Grenze kleiner Konzentrationen wird dieses Potential geschwindigkeits- und temperaturunabhängig, so daß wir im wesentlichen die Theorie von Cahn und Lücke und Stüwe erhalten. Für Temperaturen nahe der kohärenten Spinodalen nimmt bei kleinen Geschwindigkeiten die Korngrenzbeweglichkeit rasch mit zunehmender Geschwindigkeit ab; dieses Verhalten entspricht einem sehr geschwindigkeitsempfindlichen Zusammensetzungsprofil. Bei höheren Temperaturen sind diese Effekte weniger ausgeprägt. Diese Ergebnisse beziehen sich auf Geschwindig keiten unterhalb der Losreißgeschwindigkeit; der Weg zu Erweiterung dieser Theorie zu höheren Geschwindigkeiten wird angedeutet.

NOMENCLATURE

Symbol	*Definition*
α	(33a)
α_0	(30c)
β_α	(33b)
$\gamma_{\alpha\beta}$	(33c)
$\delta_{\alpha\beta}$	Kroneker δ
Δ	dilatation
$\epsilon_{\alpha\beta}$	total strain, before (1)
η	before (1)
θ	(21)
κ	Boltzmann's constant
λ	Lamé constant
λ'	effective λ, (16a)
μ	Lamé constant, shear modulus
μ'	effective μ ($\mu' = \mu$), (16b)
ν	Poisson ratio
ξ	correlation length, after (12)
ρ	mass density
σ	$c - c_0$
τ	dimensionless temperature, (22)
φ	F/A in units of μ, after (56)

† Now at: Motorola Inc. B132, 5005 E. McDowell Rd., Phoenix, AZ 85008, U.S.A.

φ'	temperature rescaled φ, (28) and (57)
$\Phi_{\alpha\beta}$	zero frequency dynamical matrix, (35)
χ	applied chemical potential field, (3)
χ_0	overall constant chemical potential, (8)
χ_e	effective chemical potential, (26)
$\chi_{e(0)}$	depth of Cahn's potential wells, (28)
ψ_α	applied force field, (3)
ω	regular solution energy parameter, (18)
Ω	atomic volume ($= a^3/4$ for f.c.c.)
a	lattice parameter
A	area of grain boundary
$\mathbf{b}$	Burgers vector
B_α	(30b)
c	mole fraction of A-atoms
c_0	average c
$C_{\alpha\beta\gamma\delta}$	elastic modulus
$C'_{\alpha\beta\gamma\delta}$	effective elastic modulus, (15)
d	amplitude of imposed distortion field, (48)
D	diffusion coefficient, (39)
D^*	self diffusion coefficient, after (39)
D'	D^* at $T = T_{ic}$, before (49)
D_0	D^* for $T \to \infty$, before (40)
$e_{\alpha\beta}$	elastic strain, before (1)
f	free energy density, before (1)
F	total drag force, (12)
$\mathscr{F}$	total free energy, (2)
$\mathscr{G}$	free energy for system with external forces, (3)
h	width of Cahn's potential wells, (28)
$\mathbf{I}_\parallel$	2×2 unit matrix, (44)
J_α	atomic flux, (6)
$\mathbf{k}$	reciprocal space vector
k_α	Cartesian component of $\mathbf{k}$
$\mathbf{k}_\parallel$	component of $\mathbf{k}$ parallel to boundary
$k_\perp$	component of $\mathbf{k}$ normal to boundary
K	gradient energy coefficient, (2)
l	dislocation spacing, before (48)
L	(45a)
m_α	momentum density, before (1)
M	mobility, (7)
$\hat{\mathbf{n}}_\parallel$	unit vector parallel to $\mathbf{k}_\parallel$
$\hat{\mathbf{n}}_\perp$	unit vector normal to boundary
p	dimensionless velocity, Peclet number, after (28) and (45e)
p'	dimensionless velocity, Peclet number, before (49)
P	(45b)
Q	heat
R	(45c)
$\mathbf{r}$	position vector
$\mathbf{r}_\parallel$	component of $\mathbf{r}$ parallel to boundary
$r_\perp$	component of $\mathbf{r}$ normal to boundary
s	rescaled σ, (51)
S	entropy
$S_{\alpha\beta}$	(55)
t	time
T	temperature
T_0	temperature of coherent spinodal
T_{ic}	temperature of incoherent spinodal
u_α	displacement field
U	internal energy
v	velocity of boundary
V	volume of crystal
w	(45f)
W	work
x_α	Cartesian component of $\mathbf{r}$
y	(45d)
Y	(52)
Z	dimensionless activation energy, (50).

Quantities with a tilde are Fourier transforms of the corresponding quantity without tilde, e.g. $\tilde{\sigma}$ is the Fourier transform of σ.

Lower case Greek subscripts refer to Cartesian components.

1. INTRODUCTION

The problem of the effect of impurities on grain boundary motion has received a good deal of theoretical attention. The first important paper was by Lücke and Detert [1], and improved versions were later published independently by Cahn [2] and by Lücke and Stüwe [3, 4]. We shall refer to this theory as the CLS theory. The model used by these workers is one in which the solute atoms interact with the boundary by a potential well which moves with the boundary. The detailed nature of the potential is not important in these theories, but the major contribution to the solute–boundary interaction is thought to be the elastic interaction caused by the atomic radius disparity between solvent and solute atoms. For small-angle boundaries, the elastic interaction arises from the strain field of the boundary dislocations. For a general boundary, the strain field is due to the elastic accommodation of the crystal lattice to the mixture of structural units each of which corresponds to a coincidence boundary with orientation near that of the general boundary [5]. The range of the elastic interaction is commensurate with the spacing of the dislocations or structural units.

For small solute concentrations, the solute atom–boundary interaction energy is independent of the presence of other solute atoms. But for large solute concentrations, two effects can influence the solute–boundary interaction. The first is that the solute atoms interact with each other, and the second is that for equilibrium situations (stationary boundary), the elastic moduli in Hooke's law are replaced by effective elastic moduli which are strongly temperature dependent. The effective elastic moduli arise in alloys with appreciable atomic-radius disparity because of the coupling between composition and strain fields [6]. The effective elastic moduli do not apply, however, to situations in which strains vary much more rapidly than the characteristic diffusional relaxation time of a composition field with similar spatial configuration. Thus, the elastic constants governing ultrasonic wave propagation are different from those governing the strain field around a static dislocation. Similarly, the nature of the strain fields near a moving grain boundary will change with velocity. For low velocities, the appropriate moduli are the effective elastic moduli; whereas for high velocities, the appropriate moduli are the ultrasonic moduli. In the language of the CLS theory, the solute–boundary interaction potential in concentrated alloys is velocity and temperature dependent at low velocities.

The grain boundary drag force consists of two parts: an intrinsic part due to dissipative processes occurring within the boundary, and an extrinsic part due to dissipative processes related to fluxes in the grains near the boundary. The main thrust of the CLS theory is the evaluation of the extrinsic part of the drag force, although the intrinsic part is also considered. In the present work, attention is confined to the extrinsic part of the drag force. The theoretical

method to be used is, however, quite different from the CLS theory, and it may be characterized as a study of coupled composition and strain fields near an alloy grain boundary.

General equations governing coupled composition and strain fields are derived in Section 2, and various special cases of and approximations to these equations are discussed. In Section 3, the relation of the present theory to the CLS theory is discussed. Section 4 is an application of Fourier techniques to analyse the linearized equations derived in Section 2 for a model of a moving grain boundary. The final section is a summary.

2. GENERAL EQUATIONS FOR COUPLED COMPOSITION AND STRAIN FIELDS

Since the thermal conductivity of an alloy is sufficiently high to keep the system isothermal for processes of interest in this work, it is the free energy density which is of interest in a thermodynamic description of the system. The free energy of a compositionally uniform (mole fraction c of A-atoms) strained and moving volume element of volume $\mathrm{d}V$ is

$$[f(c) + \tfrac{1}{2}\rho^{-1} m^2 + \tfrac{1}{2}C_{\alpha\beta\gamma\delta}e_{\alpha\beta}e_{\gamma\delta}]\mathrm{d}V.$$

Here $f(c)$ is the free energy density of an unstrained stationary volume element; it is the free energy of a homogeneous unstrained solid solution as measured by conventional means. The second term is the kinetic energy density (m_α is the momentum density, ρ is the mass density). The third term is the elastic strain energy density due to distortion of the volume element from the shape it would have in isolation from the rest of the solid solution. $C_{\alpha\beta\gamma\delta}$ are the elastic moduli as measured by, say, ultrasonic techniques, and $e_{\alpha\beta}$ is the difference between the total strain $\epsilon_{\alpha\beta}$ and the stress-free strain:

$$e_{\alpha\beta} = \epsilon_{\alpha\beta} - \eta_{\alpha\beta}\,\sigma,$$

where for cubic crystals

$$\eta_{\alpha\beta} = \eta\delta_{\alpha\beta}, \quad \eta = \frac{\mathrm{d}\ln a}{\mathrm{d}c},$$

(a is the lattice parameter) and $\sigma = c - c_0$. The average composition of the entire solid solution is c_0, i.e.

$$\int_V \sigma \mathrm{d}V = 0 \tag{1}$$

in which the integral is over the entire crystal (volume V). Lower case Greek subscripts indicate Cartesian components of vectors and tensors, and the convention of summation over repeated subscripts is employed throughout this paper. When the part of the chemical interaction between neighbouring volume elements which arises from composition differences is taken into account, the gradient energy density introduced by Cahn and Hilliard [7] is added to the free energy density, and the total free energy is written

$$\mathscr{F} = \int_V [f(c) + \tfrac{1}{2}K(\nabla c)^2 + \tfrac{1}{2}\rho^{-1}m^2 + \tfrac{1}{2}C_{\alpha\beta\gamma\delta}e_{\alpha\beta}e_{\gamma\delta}]\mathrm{d}V, \tag{2}$$

where K is the gradient energy coefficient. This is essentially the free energy used by Cahn [8] in the theory of spinodal decomposition. In the formal development which follows, it will be convenient to consider the response of the alloy to external chemical and mechanical forces. The appropriate thermodynamic potential to study is $\mathscr{G}$ where

$$\mathscr{G} = \mathscr{F} - \int_V [\chi\sigma + \psi_\alpha u_\alpha]\,\mathrm{d}V. \tag{3}$$

Here $\chi = \chi_A - \chi_B$ where χ_A is the externally applied chemical potential field for A atoms, ψ_α is the applied force field and u_α is the displacement field. Both χ and ψ_α are functions of position in the crystal.

Imagine an additional mechanical force field $\Delta\psi_\alpha$ applied to the solid solution. The condition for equilibrium, $\delta\mathscr{G} = 0$, leads to $\Delta\psi_\alpha = \delta\mathscr{G}/\delta u_\alpha$. If the force field is removed, the restoring force is $-\Delta\psi_\alpha$ and Newton's second law gives

$$\frac{\partial m_\alpha}{\partial t} = -\frac{\delta\mathscr{G}}{\delta u_\alpha}. \tag{4}$$

When (2) and (3) are used, this equation of motion becomes, for cubic crystals,

$$\rho\frac{\partial^2 u_\alpha}{\partial t^2} = C_{\alpha\beta\gamma\delta}\frac{\partial^2 u_\delta}{\partial x_\beta \partial x_\gamma} - \eta C_{\alpha\beta\gamma\gamma}\frac{\partial\sigma}{\partial x_\beta} + \psi_\alpha. \tag{5}$$

Assuming the same phenomenological diffusion law as Hilliard [9], the flux of A-atoms in the frame of reference in which the total flux vanishes is

$$J_\alpha = -c(1-c)\,M\frac{\partial}{\partial x_\alpha}\left(\frac{\delta\mathscr{G}}{\delta\sigma}\right), \tag{6}$$

where M is given by

$$M = cv_A + (1-c)\,v_B, \tag{7}$$

where v_A is the velocity of an A-atom under unit potential gradient. In the simplest model, M is independent of composition. From (2) and (3) one finds

$$\frac{\delta\mathscr{G}}{\delta\sigma} = f'(c) - K\nabla^2\sigma - \eta C_{\alpha\beta\gamma\gamma}e_{\alpha\beta} - \chi_0 - \chi, \tag{8}$$

where χ_0 is a (spatially constant) chemical potential chosen to satisfy the condition (1). If the externally applied chemical potential field is localized, the condition of equilibrium at infinity leads to $\chi_0 = f'(c_0)$. The flux must obey the equation of continuity

$$\frac{\partial\sigma}{\partial t} = -\Omega\frac{\partial J_\alpha}{\partial x_\alpha}, \tag{9}$$

where Ω is the atomic volume. Equations (5), (6), (8) and (9) are the general equations governing the coupled composition and strain fields. The model

could be made more elaborate by, for example, using composition-dependent elastic moduli, but the above model is the simplest which contains the essence of the composition-strain coupling.

A quantity which is of considerable interest in this work is the rate of entropy production. The change of entropy for the crystal is

$$\mathrm{d}S = \mathrm{d}S_i + T^{-1}\,\mathrm{d}Q,$$

where $\mathrm{d}S_i$ is the internally produced entropy ($\mathrm{d}S_i \geq 0$) and $\mathrm{d}Q$ is the heat flow from the surroundings. The change in internal energy is given by

$$\mathrm{d}U = \mathrm{d}Q + \mathrm{d}W = \mathrm{d}Q + \int_V (\chi\delta\sigma + \psi_\alpha \delta u_\alpha)\,\mathrm{d}V,$$

so

$$T\mathrm{d}S_i = T\mathrm{d}S - \mathrm{d}U + \int_V (\chi\delta\sigma + \psi_\alpha\delta u_\alpha)\,\mathrm{d}V$$

$$= -\mathrm{d}\mathscr{G} - \int_V (\sigma\delta\chi + u_\alpha\delta\psi_\alpha)\,\mathrm{d}V. \tag{10}$$

In the analysis below, we shall consider externally applied force fields which are constant in time in a frame of reference moving with uniform velocity. For such a case, the integral in (10) vanishes in the moving frame,† so that

$$T\frac{\mathrm{d}S_i}{\mathrm{d}t} = -\frac{\mathrm{d}\mathscr{G}}{\mathrm{d}t} = -\int_V \left(\frac{\delta\mathscr{G}}{\delta u_\alpha}\frac{\partial u_\alpha}{\partial t} + \rho\frac{\partial^2 u_\alpha}{\partial t^2}\frac{\partial u_\alpha}{\partial t} + \frac{\delta\mathscr{G}}{\delta\sigma}\frac{\partial\sigma}{\partial t}\right)\mathrm{d}V$$

$$= \Omega\int_V \frac{\delta\mathscr{G}}{\delta\sigma}\frac{\partial J_\alpha}{\partial x_\alpha}\,\mathrm{d}V$$

$$= -\Omega\int_V J_\alpha\frac{\partial}{\partial x_\alpha}\left(\frac{\delta\mathscr{G}}{\delta\sigma}\right)\mathrm{d}V$$

or

$$T\frac{\mathrm{d}S_i}{\mathrm{d}t} = \Omega\int_V \frac{J^2\,\mathrm{d}V}{c(1-c)M}. \tag{11}$$

In the manipulations leading to (11), equations (4), (6) and (9) were used, and the divergence theorem, assuming local equilibrium at infinity, was invoked. Equation (11) gives the total rate of heat production as, for example, the points of application of the externally applied force-fields move at uniform velocity v through the crystal. In the development below, the external force fields χ and ψ_α will be regarded as formal devices for introducing a moving local composition and strain inhomogeneity into the crystal so that (11) may be interpreted in terms of a diffusional drag force, F, on the moving inhomogeneity:

$$F = \frac{T}{v}\frac{\mathrm{d}S_i}{\mathrm{d}t} = \frac{v}{\Omega}\int_V \frac{\sigma^2\,\mathrm{d}V}{c(1-c)M}, \tag{12}$$

where we have used $J_\alpha = \Omega^{-1}\sigma v_\alpha$, which follows from (9) when the condition for steady state in the frame of reference moving with the inhomogeneity is employed.

In general, the equations governing the composition and strain fields are difficult to solve analytically, but it is possible to make several approximations which simplify their solution for the situation of interest in the present work. The most important approximation is linearization because this makes it possible to employ Fourier techniques. The gradient-energy term in (8) can be handled by Fourier methods, but it complicates the solution and has little effect when the correlation length [7] ξ is much smaller than distances over which concentration changes are appreciable.‡ The correlation length is on the order of atomic diameters or less except very near T_0 (defined below). A concentration profile near a boundary has a decay length on the order of the diffusion length, D/v, so that solutions ignoring the gradient energy are valid only for velocities sufficiently small that $\xi \ll D/v$. As we shall see, this is equivalent to velocities less than the breakaway velocity. The effect of primary interest in this work, viz., the change in elastic character of fields near a boundary, occurs in the low velocity regime so the gradient energy terms will be dropped. Another term which can be ignored is the inertial term on the left-hand side of (5). This is appreciable when the inhomogeneity moves with a velocity approaching that of sound.

The special case of equilibrium and small composition deviations is particularly easy to handle because the strain part of the problem decouples from the compositional part [6]. We derive results for this situation as a starting point for the analysis of the non-equilibrium situation which follows, and in order to define some model parameters. If the gradient energy term is ignored, equation (8) becomes for equilibrium and no external chemical forces

$$f'(c) - f'(c_0) + \sigma\eta^2 C_{\alpha\alpha\beta\beta} - \eta C_{\alpha\beta\gamma\gamma}\epsilon_{\alpha\beta} = 0. \tag{13}$$

The gradient of this yields an expression for $\partial\sigma/\partial x_\beta$ which when substituted into (5) leads to§

$$C'_{\alpha\beta\gamma\delta}\frac{\partial^2 u_\delta}{\partial x_\beta \partial x_\gamma} + \psi_\alpha = 0, \tag{14}$$

where $C'_{\alpha\beta\gamma\delta}$ is an effective elastic modulus given by

$$C'_{\alpha\beta\gamma\delta} = C_{\alpha\beta\gamma\delta} - \frac{\eta^2 C_{\alpha\beta\epsilon\epsilon}C_{\gamma\delta\zeta\zeta}}{f''(c) + \eta^2 C_{\kappa\kappa\lambda\lambda}}. \tag{15}$$

For small composition deviations, we can write

$$f'(c) \simeq f'(c_0) + \sigma f''(c_0)$$

in (8) which makes the effective elastic moduli inde-

† All partial time derivatives in the following are for coordinates fixed in the moving frame.

‡ ξ is equivalent to l in Ref. 7. ξ may also be regarded as a measure of the range of short-range order.

§ For the non-equilibrium case of an inhomogeneity moving at constant velocity, the following term is added to the left-hand side of (14):

$$[\Omega c(1-c)M(f''(c) + \eta^2 C_{\kappa\kappa\lambda\lambda})]^{-1} C_{\alpha\delta\gamma\gamma}v_\delta\sigma.$$

pendent of composition variations, and the total strains may be computed using ordinary elasticity theory but with effective elastic moduli given by (15) with $f''(c)$ replaced by $f''(c_0)$. For an isotropic crystal $C_{11} = \lambda + 2\mu$, $C_{12} = \lambda$ and $C_{44} = \mu$, where λ and μ are the Lamé constants, so (15) becomes

$$\lambda' = \lambda - \frac{\eta^2(3\lambda + 2\mu)^2}{f''(c_0) + 3\eta^2(3\lambda + 2\mu)} \tag{16a}$$

$$\mu' = \mu.$$

For a regular solution model in which

$$\Omega f(c) = \omega c(1 - c) + \kappa T[c \ln c + (1 - c) \ln (1 - c)], \tag{17}$$

where κ is Boltzmann's constant and ω is a characteristic energy parameter given by

$$\omega = \frac{\kappa T_{ic}}{2c_0(1 - c_0)}, \tag{18}$$

where T_{ic} is the temperature of the incoherent spinodal† at composition c_0, we have

$$\Omega f''(c_0) = \kappa T[c_0(1 - c_0)]^{-1} - 2\omega. \tag{19}$$

Now Cahn [8] has shown (see also below) that the coherent spinodal, T_0, is defined by the locus of

$$f''(c_0) + \frac{4\eta^2\mu(3\lambda + 2\mu)}{\lambda + 2\mu} = 0 \tag{20}$$

† The incoherent spinodal is the locus of $f''(c_0) = 0$.

from which we may derive the following convenient parameter:

$$\theta = 1 - \frac{T_0}{T_{ic}} = \frac{2\eta^2\mu(3\lambda + 2\mu)\Omega}{\omega(\lambda + 2\mu)}. \tag{21}$$

It will often be convenient to present results in terms of this parameter and the dimensionless temperature

$$\tau = \frac{\kappa T}{2\omega c_0(1 - c_0)} = \frac{T}{T_{ic}}. \tag{22}$$

In the present paper, attention is confined to temperatures and compositions outside the coherent spinodal, i.e. $1 - \theta \leq \tau < \infty$. In terms of these parameters (16a) is written

$$\lambda' = \lambda - \frac{(3\lambda + 2\mu)(\lambda + 2\mu)\theta}{4\mu(\tau - 1) + 3(\lambda + 2\mu)\theta}. \tag{23}$$

At the incoherent spinodal we have $\tau = 1$ and $\lambda' = -\frac{2}{3}\mu$. This indicates that the crystal would become unstable to homogeneous dilatations at the incoherent spinodal if the average composition were not constrained to be c_0 (the bulk modulus would be $\lambda' + \frac{2}{3}\mu$). At the coherent spinodal we have $\tau = 1 - \theta$ and $\lambda' = -2\mu$, which means that any static distortion wave induced by a constant external force (or, by Fourier superposition, any induced distortion inhomogeneity) becomes unstable at T_0 (see equations 44 and 46 below). In Fig. 1 we plot λ'/λ against τ for $\lambda = 2\mu$ (corresponding to a Poisson ratio of 1/3) and various values of θ. The method of solution of an equilibrium problem for which the composition deviations are small is therefore to solve for the

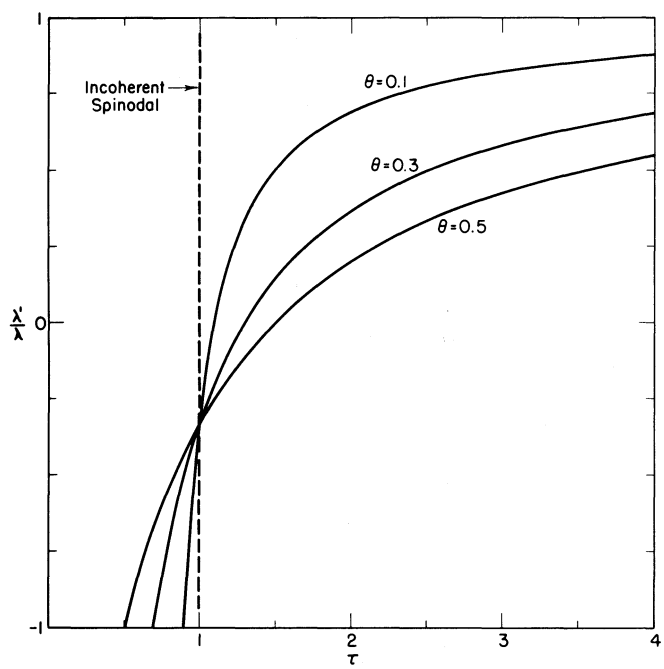

Fig. 1. The effective elastic modulus λ' in units of λ as a function of the dimensionless temperature τ for several values of $\theta = 1 - T_0/T_{ic}$, and for $\lambda = 2\mu$. The coherent spinodal occurs at τ for which $\lambda/\lambda' = -1$.

strains using conventional elasticity theory with effective elastic moduli, and then to substitute the dilatation field $\Delta = \epsilon_{11} + \epsilon_{22} + \epsilon_{33}$ into

$$\sigma = \frac{\eta(C_{11} + 2C_{12})\Delta}{f''(c_0) + 3\eta^2(C_{11} + C_{12})}$$

which follows from (13). For the isotropic regular solution this is

$$\sigma = \frac{3(\lambda + 2\mu)\theta}{4\mu(\tau - 1) + 3(\lambda + 2\mu)\theta} \frac{\Delta}{3\eta}.$$

Notice that if the dilatation field remains finite at T_0 ($\tau = 1 - \theta$) then the composition field will also remain finite. The dilatation field will remain finite at T_0 if the boundary conditions to the elasticity problem are constant strain, as opposed to constant stress, boundary conditions. The grain boundary model analyzed in Section 4 has a composition profile which is finite for equilibrium at T_0 for this reason.

When composition deviations are not small, or when equilibrium does not obtain, the equations are not as simple to solve. Large composition deviations introduce nonlinearities and the elastic and compositional parts of the problem do not decouple for general non-equilibrium situations. (However, we shall see in the following section that decoupling does obtain in the case of a grain boundary moving in a *dilute* alloy as studied by Cahn [2].) The object of the present paper is to study a situation in which the effective decoupling does not occur, namely, a steady-state non-equilibrium situation in an alloy of arbitrary composition. However, nonlinear effects will not be studied. The set of linear equations applying to the situation of interest is

$$-\eta C_{\alpha\beta\gamma\gamma} \frac{\partial\sigma}{\partial x_\beta} + C_{\alpha\beta\gamma\delta} \frac{\partial^2 u_\delta}{\partial x_\beta \partial x_\gamma} = -\psi_\alpha \qquad (24a)$$

$$[f''(c_0) + \eta^2 C_{\kappa\kappa\lambda\lambda}] \frac{\partial\sigma}{\partial x_\alpha} + \frac{v_\alpha \sigma}{c_0(1 - c_0)M\Omega} - \eta C_{\beta\gamma\delta\delta} \frac{\partial^2 u_\beta}{\partial x_\gamma \partial x_\alpha} = \frac{\partial\chi}{\partial x_\alpha}. \qquad (24b)$$

These equations follow from Equations (5), (6), (8) and (9) and they hold in a frame of reference moving at velocity v_α in which an inhomogeneity induced by external forces has reached steady state (is stationary). The following approximations have been made:

(i) Composition deviations are small.

(ii) Composition has small spatial variation on the scale of the correlation length.

(iii) The velocity of the inhomogeneity is much less than that of sound.

3. RELATION TO THE CLS THEORY

In the limit of small solute concentrations, it is apparent from equation (19) that $f''(c_0) \to \infty$. This means (see equation 15) that $C'_{\alpha\beta\gamma\delta} \to C_{\alpha\beta\gamma\delta}$, and that the velocity dependent term which would appear in (14) for a uniformly moving inhomogeneity vanishes (see footnote). Thus, the elasticity problem for an inhomogeneity moving with uniform velocity in a dilute alloy is exactly the same as for a stationary inhomogeneity in the pure metal and is therefore decoupled from the composition variations for *all* velocities. (Whereas the elastic problem is decoupled from the concentration problem in concentrated alloys at *high* velocity.) The unlinearized version of (24b) may be written by replacing c_0 by c; then using (19) we write for the isotropic regular solution

$$M\{\kappa T + c(1 - c)[3\Omega\eta^2(3\lambda + 2\mu) - 2\omega]\} \frac{\partial\sigma}{\partial x_\alpha} + v_\alpha\sigma = \Omega M c(1 - c) \frac{\partial\chi_e}{\partial x_\alpha}, \qquad (25)$$

where

$$\chi_e = \chi + \eta(3\lambda + 2\mu)\Delta, \qquad (26)$$

which is an effective chemical potential field. For small concentrations (25) becomes

$$M\kappa T \frac{\partial\sigma}{\partial x_\alpha} + v_\alpha\sigma = \Omega M c \frac{\partial\chi_e}{\partial x_\alpha}, \qquad (27)$$

which is exactly Cahn's equation with an effective interaction energy χ_e. Now we have just shown that the elasticity problem (and hence Δ) is velocity and temperature independent in the low concentration limit, so the CLS picture of diffusion in a moving velocity-independent potential is consistent and complete at low concentrations.

The situation is more complicated for arbitrary concentrations. First, equation (25) is nonlinear. Lücke and Stüwe [3, 4] took into account the nonlinearity on the right-hand side of (25), but did not take into account the non-linearity arising from solute interaction (square brackets). The other complication is that χ_e becomes concentration and hence velocity dependent, introducing further nonlinearities. It is possible to study alloy grain boundary drag by linearizing (25) about some arbitrary composition c_0, and this leads to an equation similar to (27); but with c replaced by c_0 and with χ_e a linear function of concentrations and displacements. This linearization is carried out, albeit in a different fashion, in the following section so that the model we shall study becomes formally equivalent in the low concentration limit to a *simplified* version of the CLS theory which has c replaced by c_0 in (27). It is easy to show that the solutions to the simplified CLS theory coincide with the unsimplified CLS theory when $\Omega\chi_e/\kappa T \ll 1$.

Cahn [2] and Lücke and Stüwe [3, 4] predict the phenomenon of grain boundary breakaway. This occurs when the total drag force has a local maximum for some finite velocity. This maximum is due to the extrinsic drag force component which first increases but then decreases with increasing velocity. It is not

commonly recognized, however, that this behavior in the CLS model depends on the nature of the solute–boundary interaction potential. For example, breakaway occurs for the triangular potential well studied by CLS, but not for a square well. The same behavior occurs in the simplified CLS model and one finds that the extrinsic drag force per unit area, F/A, is given by

$$F/A = c_0\Omega(\kappa T)^{-1}\,\chi_{e(0)}^2\varphi', \tag{28}$$

where

$$\varphi' = 1 - \exp(-p) \quad \text{(square well)}$$

or

$$\varphi' = \frac{2}{p}\left[\left(1-\frac{2}{p}\right)+\left(1+\frac{2}{p}\right)\exp(-p)\right]$$

(triangular well),

where $p = hv/D$, h = potential well width, and $\chi_{e(0)}$ is the maximum potential well depth. Hillert [10] has found, however, that breakaway will occur even for a square well potential if one truncates the solute "spike" at the boundary at a distance of several atomic diameters from the boundary, and that the effect of the spike truncation becomes appreciable when D/v is on the order of atomic diameters. The spike truncation procedure has its basis in the fact that concentration profiles cannot exist physically if they are narrower than a few atomic diameters, thus physically one expects breakaway always to occur at some sufficiently high velocity, no matter what the potential well shape is. The neglect of the spike–truncation procedure in the CLS model is equivalent to the neglect of the gradient energy in the present model, so from the viewpoint of the breakaway phenomenon, we see again that the model studied in this paper is valid only for $\xi \ll D/v$.

4. APPLICATION OF THE LINEAR EQUATIONS TO MOVING GRAIN BOUNDARY

(a) *The Fourier transformed equations in an isotropic alloy*

The linear equations (24) are most naturally handled by Fourier analysis, and their Fourier transforms are

$$\Phi_{\alpha\beta}\,\tilde{u}_\beta + B_\alpha\tilde{\sigma} = \tilde{\psi}_\alpha \tag{29a}$$

$$-B_\alpha\tilde{u}_\alpha + \alpha_0\,\tilde{\sigma} = \tilde{\chi}, \tag{29b}$$

where

$$\Phi_{\alpha\beta} = C_{\alpha\gamma\beta\delta}\,k_\gamma k_\delta \tag{30a}$$

$$B_\alpha = -i\eta C_{\alpha\beta\gamma\gamma}k_\beta \tag{30b}$$

$$\alpha_0 = f''(c_0) + \eta^2\,C_{\alpha\alpha\beta\beta} + Kk^2 + ik_\alpha\,v_\alpha\,[c_0(1-c_0)M\Omega k^2]^{-1}, \tag{30c}$$

where k_α is a cartesian coordinate in reciprocal space and where the Fourier transform of, say, σ is given by

$$\tilde{\sigma} = \int_V \sigma\exp(ik_\alpha x_\alpha)\,dV. \tag{31}$$

We have temporarily reintroduced the gradient energy contribution in α_0. Equations (29) may be inverted to find the composition and strain fields which arise in response to the chemical and mechanical force fields $\tilde{\chi}$ and $\tilde{\psi}_\alpha$:

$$\tilde{\sigma} = \alpha^{-1}\tilde{\chi} + \beta_\alpha\tilde{\psi}_\alpha \tag{32a}$$

$$\tilde{u}_\alpha = -\beta_\alpha\tilde{\chi} + \gamma_{\alpha\beta}\tilde{\psi}_\beta, \tag{32b}$$

where

$$\alpha = f''(c_0) + \eta^2\,C_{\alpha\alpha\beta\beta} + B_\alpha\,\Phi_{\alpha\beta}^{-1}\,B_\beta + Kk^2 + ik_\alpha v_\alpha[c_0(1-c_0)M\Omega k^2]^{-1} \tag{33a}$$

$$\beta_\alpha = \alpha^{-1}\,\Phi_{\alpha\beta}^{-1}\,B_\beta \tag{33b}$$

$$\gamma_{\alpha\beta} = \Phi_{\alpha\beta}^{-1} - \alpha\beta_\alpha\beta_\beta. \tag{33c}$$

For simplicity's sake, calculations will be performed for an elastically isotropic solid solution. Results will be given both for an arbitrary free energy density, and for the regular solution model defined in Section 2. For the isotropic case

$$B_\alpha = -i(3\lambda + 2\mu)\,k_\alpha \tag{34}$$

$$\Phi_{\alpha\beta} = \mu k^2\,\delta_{\alpha\beta} + (\lambda+\mu)k_\alpha\,k_\beta. \tag{35}$$

It is easy to verify that

$$\Phi_{\alpha\beta}^{-1} = \frac{1}{\mu k^2}\left(\delta_{\alpha\beta} - \frac{\lambda+\mu}{\lambda+2\mu}\frac{k_\alpha k_\beta}{k^2}\right) \tag{36}$$

and consequently to demonstrate that

$$B_\alpha\,\Phi_{\alpha\beta}^{-1}\,B_\beta = -\eta^2(3\lambda+2\mu)^2\,(\lambda+2\mu)^{-1}.$$

Thus at $k = 0$ and $v = 0$, α is given by

$$\alpha(0) = f''(c_0) + 4\eta^2\mu(3\lambda+2\mu)(\lambda+2\mu)^{-1} \tag{37a}$$

$$= 2\omega\Omega^{-1}(\tau - 1 + \theta), \tag{37b}$$

where the second equality is for the regular solution model. $\alpha(0)$ vanishes at the coherent spinodal (see equation 20). At this point, we drop the gradient energy contribution from (33a) but note that for other applications of the equations (such as grain-boundary drag for $D/v < \xi$) it may be necessary to retain it. Equation (33a) becomes

$$\alpha = \alpha(0)\,[1 + ik_\alpha\,v_\alpha\,(Dk^2)^{-1}], \tag{38}$$

where

$$D = \alpha(0)\,c_0\,(1-c_0)\,M\Omega. \tag{39}$$

If in addition to the isotropic regular solution assumption, we assume a model in which M is independent of composition, then $M = D^*/\kappa T$, where D^* is the self-diffusion coefficient in the pure metals (both

have the same D^*). If $D^* = D_0 \exp(-Q/\kappa T)$ where D_0 is a constant, then

$$D = D_0 [1 - (1 - \theta)/\tau] \exp(-Q/\kappa T), \quad (40)$$

where we have used equations (37b) and (22). We also have

$$\beta_\alpha = -\frac{i\eta(3\lambda + 2\mu) k_\alpha}{\alpha(0)(\lambda + 2\mu)(k^2 + ik_\beta v_\beta D^{-1})} \quad (41)$$

and

$$\gamma_{\alpha\beta} = \Phi_{\alpha\beta}^{-1} + \frac{\eta^2(3\lambda + 2\mu)^2 k_\alpha k_\beta}{\alpha(0)(\lambda + 2\mu)^2 k^2 (k^2 + ik_\gamma v_\gamma D^{-1})}. \quad (42)$$

For $v = 0$ it can be shown that $\gamma_{\alpha\beta}$ has exactly the form of (36) but with λ replaced by λ'.

(b) *A planar distortion model of a symmetric grain boundary*

Computer simulations of grain boundary structure and energy [11] have revealed that although the energy is sensitive to the precise form of the interatomic potentials, the structure is not. This is consistent with the notion that the grain boundary structure problem can be regarded in a first approximation as one of finding the best fit of arrays of "hard balls". It is therefore reasonable to simulate the displacement field near a grain boundary by the displacement field in a semi-infinite crystal with an externally imposed two dimensional distortion field (not force-field) on its free surface. The strain field on each side of the grain boundary can be simulated in this way, but not necessarily by the *same* two dimensional distortion field. For example, one side of a symmetric tilt boundary will have a strain field, one Fourier component of which can be simulated by an imposed two-dimensional distortion field with polarization normal to the free surface (see below). Because of the symmetry, the other side of the boundary must have its corresponding strain field Fourier component simulated by an imposed two-dimensional distortion field of opposite sign. We shall call this a "physical simulation" (see Fig. 2). On the other hand, for the mathematical methods used in the present paper it will be more convenient to use a mathematical simulation in which the imposed distortion field is applied to a plane bisecting an infinite crystal. This necessarily corresponds to applying *the same* two-dimensional distortion field to the surfaces of the semi-infinite crystals defined by the plane. Any strain field simulated in this way by an imposed two-dimensional distortion field with polarization normal to the plane cannot have the reflection symmetry required of the physical symmetrical boundary. However, each normally polarized Fourier component in this mathematical simulation generates a distortion field on one side of the boundary which is related to the corresponding field in the physical simulation by a shift of half a wavelength parallel to the wavevector of the imposed two-dimensional distortion on the plane as in Fig. 2.

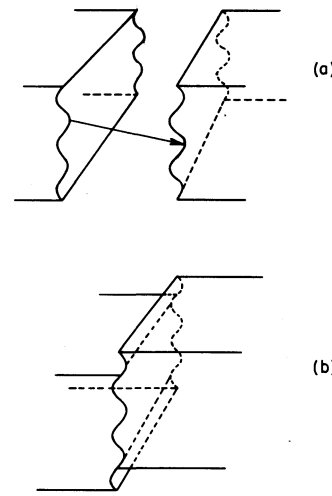

Fig. 2. (a) Physical simulation of a Fourier component of the strain field near a symmetric boundary by imposing two-dimensional distortions on the free surfaces of semi-infinite crystals. (b) The corresponding mathematical simulation obtained by the translation indicated in (a).

When the polarization vector of the imposed two-dimensional distortion field is in the plane of the boundary there is no distinction between the physical and the mathematical simulations because the mathematical simulation will have the physical reflection symmetry required of a symmetrical boundary. Thus, even though the total distortion field in the mathematical simulation may not have the reflection symmetry of the physical symmetrical boundary, each Fourier component has reflection, or reflection plus translation, symmetry in the boundary plane. Since the present model is linear, calculations such as the integration of (12) may be performed separately for each Fourier component. Taking each Fourier component separately, it is fairly obvious that the non-physical translations introduced by using the mathematical simulation depicted in Fig. 2 will have no effect on the value of the integral in (12). By superposition this is also true when all the Fourier components are taken together. The conclusion is that the mathematically convenient but unsymmetrical simulation of the strain fields obtained by imposing a two-dimensional distortion field on a plane bisecting an infinite crystal will yield the correct value for F (via 12) corresponding to a symmetrical physical boundary in which normally polarized Fourier components are related to the corresponding Fourier components in the mathematical simulation as in Fig. 2.

Consider a plane, which we shall call the defect plane, cutting through an infinite crystal and moving with velocity v, and let there be an external mechanical force field applied in this plane. Let $\hat{\mathbf{n}}_\perp$ be a unit vector in the direction of the velocity (normal to the plane). We can write a position vector in real space as $\mathbf{r} = \mathbf{r}_\parallel + \hat{\mathbf{n}}_\perp r_\perp$, where $\mathbf{r}_\parallel$ is the component of $\mathbf{r}$ parallel to the planar defect. We take the origin of coordinates to lie in the defect plane. $\mathbf{k}$, $\mathbf{k}_\parallel$ and $k_\perp$

have similar definitions in k-space. Also, $\hat{\mathbf{n}}_{\|}$ is a unit vector parallel to $\mathbf{k}_{\|}$. With these definitions, we can say that the defect plane is at $r_{\perp} = 0$, that $\tilde{\chi} = 0$, and $\tilde{\psi}_{\alpha}(\mathbf{k})$ is independent of $k_{\perp}$, i.e. $\tilde{\psi}_{\alpha}(\mathbf{k}) = \tilde{\psi}_{\alpha}(\mathbf{k}_{\|})$. The two dimensional Fourier transform of $u_{\alpha}(\mathbf{r})$ in a plane parallel to the defect plane is given by the $k_{\perp}$-inverse Fourier transform of $\tilde{u}_{\alpha}(\mathbf{k})$:

$$\tilde{u}_{\alpha}(\mathbf{k}_{\|}, r_{\perp}) = (2\pi)^{-1} \int_{-\infty}^{+\infty} \tilde{u}_{\alpha}(\mathbf{k}) \exp(-ik_{\perp} r_{\perp})\, dk_{\perp}.$$

When the $k_{\perp}$-inverse Fourier transform is applied to equations (32) and the $k_{\perp}$-independence of $\tilde{\psi}_{\alpha}$ is taken into account, we find

$$\tilde{u}_{\alpha}(\mathbf{k}_{\|}, r_{\perp}) = \gamma_{\alpha\beta}(\mathbf{k}_{\|}, r_{\perp})\, \gamma^{-1}_{\beta\gamma}(\mathbf{k}_{\|}, 0)\, \tilde{u}_{\gamma}(\mathbf{k}_{\|}, 0) \quad (43a)$$

$$\tilde{\sigma}(\mathbf{k}_{\|}, r_{\perp}) = \beta_{\alpha}(\mathbf{k}_{\|}, r_{\perp})\, \gamma^{-1}_{\alpha\beta}(\mathbf{k}_{\|}, 0)\, \tilde{u}_{\beta}(\mathbf{k}_{\|}, 0). \quad (43b)$$

These expressions relate the composition and displacement fields near the defect plane to the two-dimensional Fourier transform of the imposed displacement field at $r_{\perp} = 0$, viz $\tilde{u}_{\alpha}(\mathbf{k}_{\|}, 0)$. It is a long but straightforward exercise in complex analysis to find the following $k_{\perp}$-projection of $\gamma_{\alpha\beta}$:

$$\gamma_{\alpha\beta}(\mathbf{k}_{\|}, 0) = (2\pi)^{-1} \int_{-\infty}^{+\infty} \gamma_{\alpha\beta}(\mathbf{k})\, dk_{\perp},$$

and to find its matrix inverse. The result is

$$\gamma^{-1}_{\alpha\beta}(\mathbf{k}_{\|}, 0) = 2\mu\, k_{\|} \left[\begin{array}{c|c} \mathbf{I}_{\|} + L\, \hat{\mathbf{n}}_{\|} \hat{\mathbf{n}}_{\|} & iP\hat{\mathbf{n}}_{\|} \\ \hline iP\, \hat{\mathbf{n}}_{\|} & R \end{array}\right], \quad (44)$$

where $\mathbf{I}_{\|}$ is a 2×2 unit matrix and

$$L = \frac{\lambda + \mu - 2(\lambda + 2\mu)\, w(1 + p^2)^{-\frac{1}{2}}}{\lambda + 3\mu + 2(\lambda + 2\mu)\, w(1 + p^2)^{-\frac{1}{2}}} \quad (45a)$$

$$P = \frac{w}{y} \frac{p}{1 + p^2 + (1 + p^2)^{\frac{1}{2}}} \quad (45b)$$

$$R = \frac{1}{y}\left[\frac{\lambda + 3\mu}{2(\lambda + 2\mu)} + \frac{w}{(1 + p^2)^{\frac{1}{2}}}\right] \quad (45c)$$

$$y = \frac{(\lambda + 3\mu)^2}{4(\lambda + 2\mu)^2} + \frac{(\lambda + 3\mu)}{(\lambda + 2\mu)} \frac{w}{(1 + p^2)^{\frac{1}{2}}} + \frac{2w^2}{1 + p^2 + (1 + p^2)^{\frac{1}{2}}}, \quad (45d)$$

where p is a Peclet number or dimensionless velocity given by

$$p = v/(2Dk_{\|}) \quad (45e)$$

and

$$w = \frac{\eta^2(3\lambda + 2\mu)^2 \mu}{2\alpha(0)\,(\lambda + 2\mu)^2} = \frac{(3\lambda + 2\mu)}{8(\lambda + 2\mu)} \frac{\theta}{(\tau - 1 + \theta)}, \quad (45f)$$

where the second equality is for the regular solution model. It is not difficult to show that

$$\lim_{p \to \infty} R = \lim_{p \to \infty} (1 + L) = 2(\lambda + 2\mu)/(\lambda + 3\mu) \quad (46a)$$

and

$$\lim_{p \to \infty} P = 0. \quad (46b)$$

The results for the $p \to 0$ limits have the same form but with λ replaced by λ' in (46a). It is also possible to use complex analysis to find $\beta_{\alpha}(\mathbf{k}_{\|}, r_{\perp})$, and the result is:

$$\boldsymbol{\beta}(\mathbf{k}_{\|}, r_{\perp}) = -\frac{i\eta(3\lambda + 2\mu)}{2\alpha(0)\,(\lambda + 2\mu)} \frac{\exp[-(1 + p^2)^{\frac{1}{2}} k_{\|} r_{\perp}]}{(1 + p^2)^{\frac{1}{2}}} \times [\hat{\mathbf{n}}_{\|} - i\hat{\mathbf{n}}_{\perp}(p + (1 + p^2)^{\frac{1}{2}})]\, (r_{\perp} > 0) \quad (47a)$$

and

$$\boldsymbol{\beta}(\mathbf{k}_{\|}, r_{\perp}) = -\frac{i\eta(3\lambda + 2\mu)}{2\alpha(0)\,(\lambda + 2\mu)} \times \frac{\exp[((1 + p^2)^{\frac{1}{2}} - p)k_{\|} r_{\perp}]}{(1 + p^2)^{\frac{1}{2}}} \times [\hat{\mathbf{n}}_{\|} - i\hat{\mathbf{n}}_{\perp}(p - (1 + p^2)^{\frac{1}{2}})](r_{\perp} < 0). \quad (47b)$$

Equations (44) and (47) enable one to compute the composition profile near a moving boundary via equation (43b). The corresponding displacement field is not of direct interest, so $\gamma_{\alpha\beta}(\mathbf{k}_{\|}, r_{\perp})$ will not be given explicitly.

A realistic grain boundary will have strain fields which are simulated by a complicated two-dimensional distortion field $u_{\alpha}(\mathbf{r}_{\|}, 0)$. In the present analysis, we shall use the simplest model grain boundary which demonstrates the phenomenon of interest. It is possible to use (43a) for the special case of a stationary boundary in a pure metal to find the two-dimensional imposed distortion field which gives a strain field in the $r_{\perp} > 0$ grain which is asymptotically identical (as $r_{\perp} \to \infty$) with the strain field due to an array of edge dislocations comprising a tilt boundary [12]. If the dislocations have Burgers vector $\mathbf{b}$ and spacing $l = 2\pi/q_{\|}$ where $\mathbf{q}_{\|}$ has a direction normal to the dislocations in the plane of the boundary,

$$\mathbf{u}(\mathbf{r}_{\|}, 0) = d(\hat{\mathbf{n}}_{\|} \cos \mathbf{q}_{\|} \cdot \mathbf{r}_{\|} + \hat{\mathbf{n}}_{\perp} \sin \mathbf{q}_{\|} \cdot \mathbf{r}_{\|}), \quad (48)$$

where

$$d = \frac{\lambda + 3\mu}{\lambda + 2\mu} \frac{b}{2\pi} = 0.20b,$$

where the second equality holds for $\nu = 1/3$. The two-dimensional distortion field simulating the $r_{\perp} \to -\infty$ behavior of the strain field is the same as (48), but with $-\hat{\mathbf{n}}_{\perp}$ replacing $\hat{\mathbf{n}}_{\perp}$. The model given by (48) is not expected to give more than a crude approximation to the extrinsic properties of a symmetric tilt boundary. The main purpose of the asymptotic matching is to give an estimate of the magnitude of d to be expected in the dominant Fourier component of a model of a general grain boundary. Equation (48) is the model in which the grain boundary drag and composition profiles will be calculated below.

(c) *Composition profile and drag force for the model boundary*

It is of considerable interest to study the drag force and composition profiles as a function of a dimen-

sionless velocity for various temperatures. p, defined in equation (45e) is a dimensionless velocity, but it depends on temperature through D, so it is not a useful parameter for this purpose. We therefore arbitrarily define a new Peclet number

$$p' = v/2D'k_{\|},$$

where D' is given by

$$D' = c_0 D_B^* + (1 - c_0) D_A^*,$$

where D_A^* and D_B^* are the tracer diffusivities at composition c_0 at the incoherent spinodal. Thus p in Equations (45), (47), etc. is related to p', the dimensionless velocity of interest, by $p = p'\,(D'/D)$. In the model described above $D' = D_0 \exp(-Q/\kappa T_{ic})$ so, from (39),

$$p = p' \frac{\tau}{\tau - 1 + \theta} \exp\left[Z\left(\frac{1}{\tau} - 1\right)\right], \tag{49}$$

where

$$Z = Q/\kappa T_{ic}. \tag{50}$$

Z may be regarded as a dimensionless activation energy. To compute the dimensionless drag forces and composition profiles defined below in the isotropic regular solution composition independent mobility model, it is necessary to specify θ, λ/μ, and Z. Plots of drag force, etc., in the present paper are all for $\theta = 0.3$, $\lambda/\mu = 2$, and $Z = 1$.

The composition profile corresponding to (48) may be computed by taking the two-dimensional inverse transform of (43b) using (44) and (47) and the Fourier transform of (48). It is convenient to present the results in terms of a rescaled composition deviation defined by

$$s = \frac{\eta\sigma}{2dq_{\|}}. \tag{51}$$

The concentration profiles are

$$s(\mathbf{r}_{\|}, r_{\perp}) = -\frac{\mu\eta^2(3\lambda + 2\mu)\,Y}{\alpha(0)\,(\lambda + 2\mu)} \sin(\mathbf{q}_{\|}\cdot\mathbf{r}_{\|})$$

$$= -\frac{\theta Y}{8(\tau - 1 + \theta)} \sin(\mathbf{q}_{\|}\cdot\mathbf{r}_{\|}), \tag{52a}$$

where the second equality is for the regular solution model and where (p is given by (45e) with $k_{\|} \to q_{\|}$).

$$Y = (1 + p^2)^{-\frac{1}{2}}\{1 + L - P + [(1 + p^2)^{\frac{1}{2}} + p] \times (R + P)\}\exp[-(1 + p^2)^{\frac{1}{2}} q_{\|} r_{\perp}] \quad (r_{\perp} > 0) \tag{52b}$$

$$Y = (1 + p^2)^{-\frac{1}{2}}\{1 + L + P + [(1 + p^2)^{\frac{1}{2}} - p] \times (R - P)\}\exp[((1 + p^2)^{\frac{1}{2}} - p) q_{\|} r_{\perp}] \quad (r_{\perp} < 0). \tag{52c}$$

An interesting special case of these equations is that at $v = 0$ and $T = T_0$:

$$s(\mathbf{r}_{\|}, r_{\perp}) = -\frac{2(\lambda + 2\mu)}{(3\lambda + 2\mu)} \exp(-q_{\|}|r_{\perp}|)\sin(\mathbf{q}_{\|}\cdot\mathbf{r}_{\|}).$$

For $\lambda = 2\mu$ the amplitude of this function is unity.

Figure 3 gives plots of rescaled composition deviation as a function of distance from the boundary one quarter of the way between dislocations for several velocities and for two temperatures. One of the temperatures is just above the coherent spinodal and the other is somewhat higher but still below the incoherent spinodal. Three features are apparent: (i) As the temperature increases, the amplitude of the zero velocity profile decreases from 1 at $T = T_0$. (ii) The composition profile is more sensitive to changes in velocity as $T \to T_0$. (iii) There is an apparent discontinuity in composition across the boundary for non-zero velocity. Physically, the concentration profiles are continuous across the boundary, but the curves in Fig. 3 differ from the physical profiles only within a distance ξ of the boundary. Since the case we are considering is $D/v \gg \xi$, this distance is negligible in Fig. 3, and profiles are what one would observe in any experiment with a spatial resolution much worse than ξ, which is usually the case. Figure 4 gives plots of the amplitudes of the profiles just in front and just behind the boundary as a function of velocity for two temperatures. The apparent macroscopic composition discontinuity increases more rapidly with velocity at temperatures nearer the coherent spinodal. This is an example of velocity-dependent deviations from equilibrium (apparent) interface concentrations. Apparent velocity-dependent concentration deviations obtained by looking at the profiles with a resolution much worse than ξ were also studied in a different model by Langer and Sekerka [13]. We should point out that the composition profiles given by equations (52) give no net composition change at the boundary, just a redistribution along it. If one were to include non-linear concentration effects, which are almost certainly important in many cases, then there is a possibility of a net composition change at the boundary.

To leading order in the composition deviations, equation (12) may be written

$$F = \frac{\alpha(0)v}{D}\int_V \sigma^2 \mathrm{d}V = \frac{\alpha(0)v}{8\pi^3 D}\int \sigma(\mathbf{k})\,\sigma(-\mathbf{k})\,\mathrm{d}^3k, \tag{53}$$

where we have used (39) and Parseval's theorem. Using the $r_{\perp}$-Fourier transform of equation (43b), we can write (53) as

$$F = \frac{\alpha(0)v}{4\pi^2 D}\int \mathrm{d}^2k_{\|}\,\tilde{u}_{\alpha}(\mathbf{k}_{\|}, 0)\,\gamma^{-1}_{\alpha\beta}(\mathbf{k}_{\|}, 0) \times \left[\frac{1}{2\pi}\int_{-\infty}^{\infty} \mathrm{d}k_{\perp}\beta_{\beta}(\mathbf{k})\beta_{\gamma}(-\mathbf{k})\right] \times \gamma^{-1}_{\gamma\delta}(-\mathbf{k}_{\|}, 0)\tilde{u}_{\delta}(-\mathbf{k}_{\|}, 0).$$

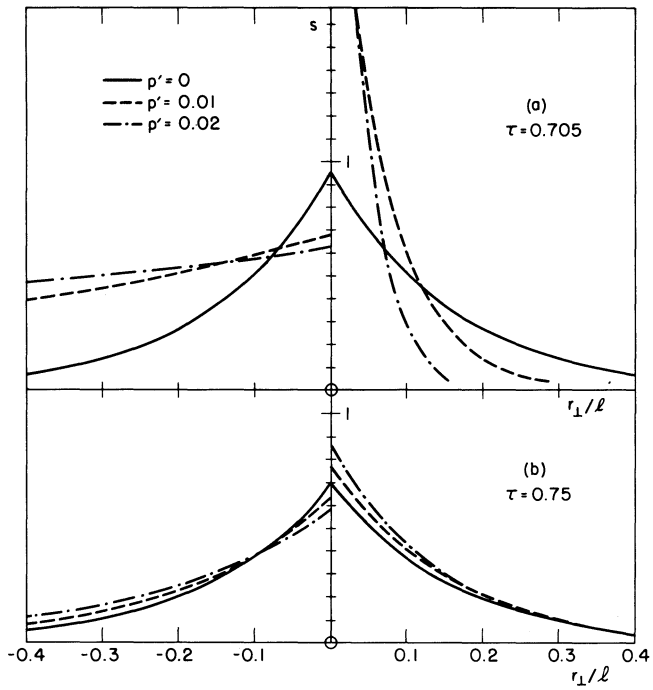

Fig. 3. Rescaled composition deviation s as a function of distance from the boundary $r_\perp/l$ one quarter of the way between dislocations ($\mathbf{q}\| \cdot \mathbf{r}\| = -\pi/2$) for several dimensionless velocities p' and for two dimensionless temperatures τ. Note the increasing sensitivity of the composition profile to changes in velocity as one nears the coherent spinodal ($\tau = 0{\cdot}7$). Model parameters: $\theta = 0{\cdot}3$, $Z = 1$, $\lambda/\mu = 2$. The boundary is moving to the right.

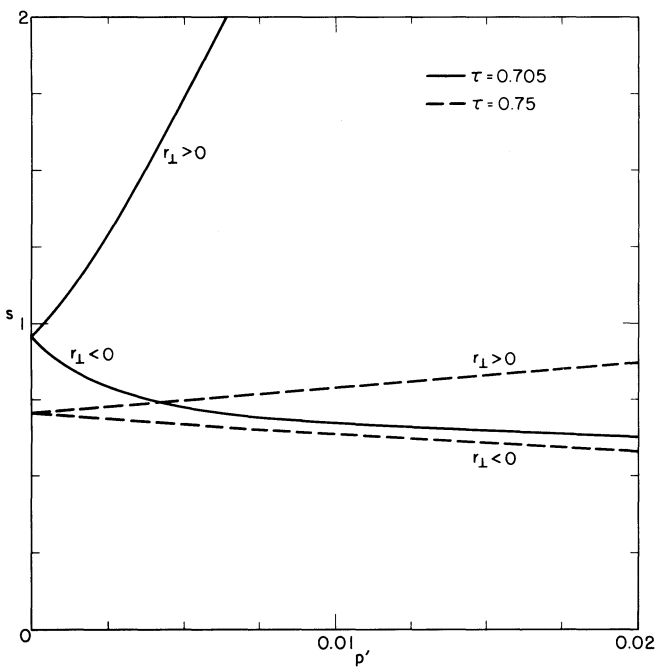

Fig. 4. Rescaled composition deviation s at the boundary one quarter of the way between dislocations as a function of dimensionless velocity p' for two temperatures. Upper curves are compositions just in front of the boundary, while the lower curves are compositions just behind it. These curves give the velocity-dependent departures of interface compositions from equilibrium ($p' = 0$), and show that such departures are greater near the coherent spinodal. Model parameters: $\theta = 0{\cdot}3$, $Z = 1$, $\lambda/\mu = 2$.

Evaluation of the Fourier $k_\perp$-projection in the square brackets and multiplication on the left and right by $\gamma^{-1}_{\alpha\beta}(\mathbf{k}_\parallel, 0)$ leads to

$$F = \frac{2\mu v w}{D}\frac{1}{4\pi^2}\int \tilde{u}_\alpha(\mathbf{k}_\parallel, 0)\, S_{\alpha\beta}(\mathbf{k}_\parallel)\tilde{u}_\beta(-\mathbf{k}_\parallel, 0)\, \mathrm{d}^2 k_\parallel, \quad (54)$$

where

$$S_{\alpha\beta}(\mathbf{k}_\parallel) = k_\parallel(1+p^2)^{-\frac{1}{2}} \times \left[\begin{array}{c|c} [(1+L)^2 + P^2]\hat{\mathbf{n}}_\parallel\hat{\mathbf{n}}_\parallel & -iP[1+L-R]\hat{\mathbf{n}}_\parallel \\ \hline iP[1+L-R]\hat{\mathbf{n}}_\parallel & P^2+R^2 \end{array}\right]. \quad (55)$$

Equation (54) may be used to compute the extrinsic drag on any model boundary. In particular, the grain boundary model given by (48) leads to

$$\varphi(dq_\parallel)^{-2} = 2wp(1+p^2)^{-\frac{1}{2}}[(1+L)^2 + R^2 + 2P^2], \quad (56)$$

where φ is the drag force per unit area of boundary expressed in units of the shear modulus, i.e.

$$F = \varphi\mu A$$

and where now $p = v/(2Dq_\parallel)$. Plots of

$$\varphi' = \frac{\varphi(\tau - 1 + \theta)}{(dq_\parallel)^2\theta} \quad (57)$$

vs p' are given in Fig. 5. The factor $(\tau - 1 + \theta)/\theta$ removes a temperature dependence analogous to the coefficient of φ' in equation (28). The shape of the curves in Fig. 5 is similar to φ' for the square-well potential in the modified CLS theory, and it is apparent that breakaway does not occur. In the low velocity region indicated by the box near the origin in Fig. 5, φ' becomes a complicated function of p' and τ with the curves for different τ crossing each other in a confusing fashion. This confusion can be eliminated by plotting $\varphi(dq_\parallel)^{-2}$ given by (56) with w given by (45f) (second equality) vs p' and Fig. 6 gives such plots. A particularly interesting feature of these plots is that the slope of these curves grows without limit as $T \to T_0$ (i.e. $\tau \to 1 - \theta$) for *finite* p', but for $p' = 0$ the slope approaches a finite value as $T \to T_0$. In fact the slope at $p' = 0$ is given by

$$\frac{1}{(dq_\parallel)^2}\frac{\mathrm{d}\varphi}{\mathrm{d}p'} = \frac{2(\lambda+2\mu)(3\lambda+2\mu)\theta\tau}{(\lambda+3\mu)^2} \times \left[\tau - 1 + \theta + \frac{(3\lambda+2\mu)}{4(\lambda+3\mu)}\theta\right]^{-2} \times \exp\left[Z\left(\frac{1}{\tau} - 1\right)\right].$$

This is plotted in Fig. 7.

It is possible to give a physical interpretation of the interesting features of Figs. 3–7. As $T \to T_0$, $\lambda' \to -2\mu$ and for a static boundary $\gamma^{-1}_{\alpha\beta}(\mathbf{k}_\parallel, 0) \to 0$ (see equations 44 and 46), while on the other hand $\beta_\alpha(\mathbf{k}_\parallel, r_\perp) \to \infty$ (see equation 47 and note that $\alpha(0) \to 0$ as $T \to T_0$). Thus, it turns out that the reduction in stresses as $T \to T_0$ (due to the effective elastic softening) induced by the imposed two-dimensional distortion field is balanced by an increase in susceptibility of composition deviations to the the stresses so that there is a finite concentration profile at

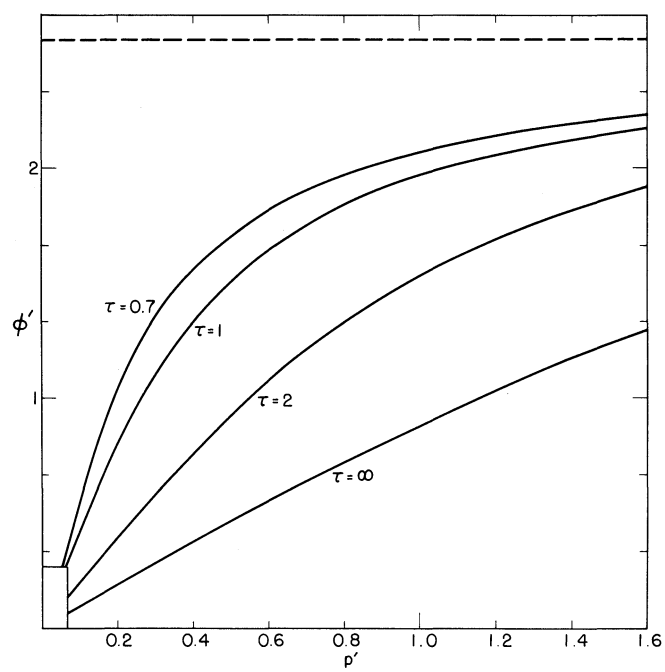

Fig. 5. A temperature rescaled drag force φ' (see equation 57) as a function of velocity for several temperatures. All curves asymptote to the horizontal broken line which shows that breakaway does not occur in this model. Model parameters: $\theta = 0{\cdot}3$, $Z = 1$, $\lambda/\mu = 2$.

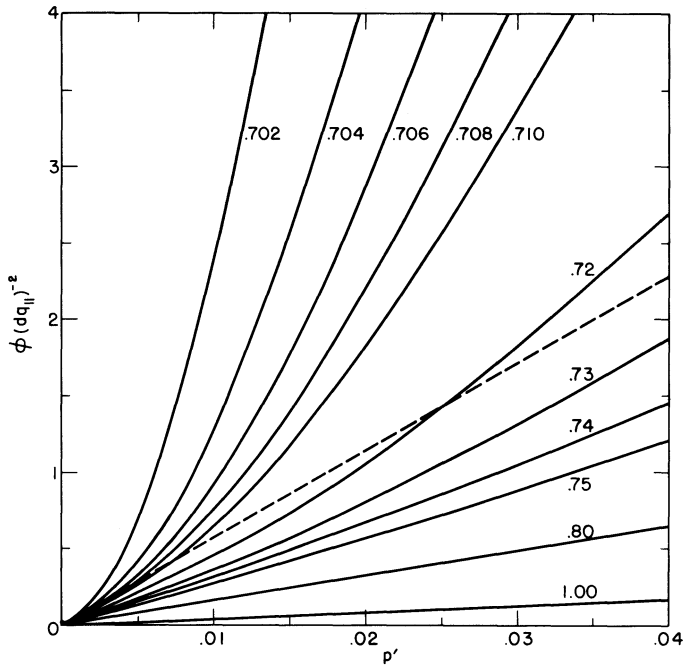

Fig. 6. Dimensionless drag force $\varphi(dq_{\parallel})^{-2}$ as a function of velocity for several temperatures. The slope at $p' = 0$ has an upper limit indicated by the broken line. As the coherent spinodal is approached ($\tau \rightarrow 0{\cdot}7$) the slope of the curve begins to depend strongly on velocity, indicating a rapid decrease in mobility with increasing velocity at low velocities near the coherent spinodal. The curves are labelled with values of τ.

$T = T_0$, and a consequent finite grain boundary mobility (see equation 12). As the boundary begins to move, the effective elastic constants λ' tend to be replaced by λ so that the induced stresses increase as the boundary velocity increases. However, the susceptibility will remain high if T is near T_0 so that the concentration profile will be particularly sensitive to increases in velocity, for low velocities, and we can expect a rapid decrease in grain boundary mobility† with velocity. For temperatures considerably higher than T_0 λ' is not so different from λ so the sensitivity of the composition profile and mobility to changes in velocity will be less than for $T \approx T_0$.

† The grain boundary mobility is proportional to the reciprocal of the slopes of the curves in Figure 6.

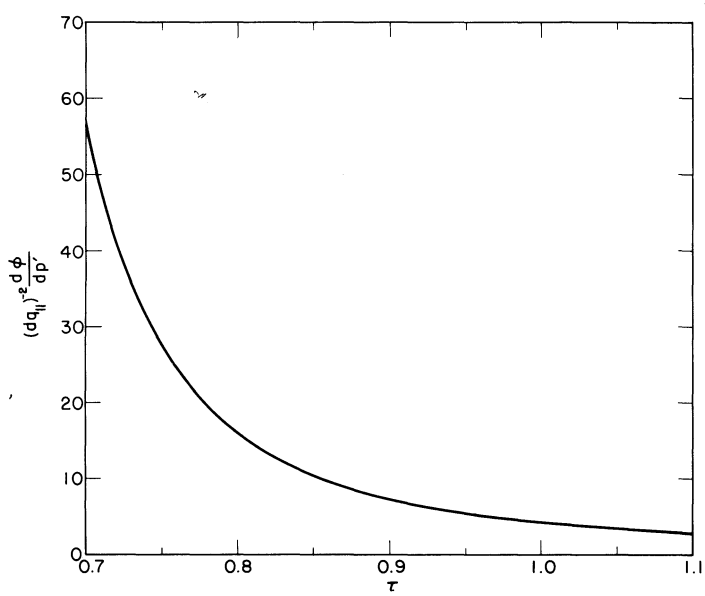

Fig. 7. Inverse mobility at $p' = 0$ as a function of temperature, showing a finite mobility at the coherent spinodal as $p' \rightarrow 0$.

5. SUMMARY AND CONCLUSIONS

In a concentrated alloy with appreciable atomic radius disparity, the coupling of the concentration and strain fields leads to interesting extrinsic grain boundary properties which are not observed in dilute alloys.† When T is near T_0 grain boundary mobility is sensitive to velocity at small velocities, decreasing rapidly with increasing velocity. The composition profile is correspondingly sensitive to velocity. At higher temperatures, the mobility is not as sensitive to velocity, and the composition profile is less polarizable. These properties can be seen in Figs. 3 and 6. This behavior may be understood qualitatively in terms of the effective elastic constants. The character of the strain field near the boundary changes as velocity increases because composition variations have less time to relax, and consequently the appropriate elastic constants which relate the imposed strains to the dilatational stresses which induce composition deviations change from λ', μ' to λ, μ. The effect is less pronounced at higher temperatures because $\lambda' \to \lambda$ as $T \to \infty$ (see Fig. 1). The character of the strain field is also independent of velocity and temperature in the low concentration limit because we also have $\lambda' \to \lambda$ in this limit. This leads to the concept of a temperature and velocity-independent solute-grain boundary interaction potential for dilute alloys. This interaction potential may be identified with the potential in a simplified version of the CLS theory, thus establishing the relation between the present theory and the CLS theory.

The curves in Fig. 5 do not peak at a finite velocity so it is apparent that the phenomenon of breakaway does not occur for the model studied in the present work. Physically, however, breakaway must occur at a sufficiently high velocity. This will be due either to the effect of the gradient energy or, at some lower velocity, to the specific nature of the solute–boundary interaction potential, as in the case of the triangular potential well in the CLS theory. In terms of the concentration profiles, the neglect of the gradient energy means that the occurrence of discontinuities in concentration at the boundary may be regarded as a result of viewing the concentration profiles on a macroscopic scale on which the correlation length is invisible. On this macroscopic scale, the composition discontinuities may be interpreted as a special case of velocity-dependent departures from equilibrium interface compositions (see Fig. 4). However, for velocities such that the diffusion length D/v is comparable with the correlation length, such interpretations are impossible and one cannot avoid including the gradient energy in the model. Thus, the model studied in the present paper is valid when $D/v \gg \xi$, and to remove this restriction, one must include the gradient energy in the model. It is still possible to employ Fourier techniques when the gradient energy is included, and although the analysis remains tractable, it is more complicated.

The linearization of the general equations makes it possible to employ Fourier techniques and to use the superposition principle to derive general results such as equation (54) for grain boundary properties in the linear regime. However, nonlinearities will be important, for example, at relatively low temperatures near dislocation cores. Chemical nonlinearities (i.e. $f(c)$ non-parabolic) will probably lead to a net accumulation of one species at the boundary due to strains. The linear theory studied in the present paper gives a redistribution along the boundary, but no net segregation to the boundary. (The linear theory can give a net accumulation at the boundary if there is a *chemical* component χ to the externally applied force fields—this was not studied in the present paper.) Although nonlinearities are very interesting, the mathematics is largely intractable except perhaps for some very idealized models, or by a resort to numerical analysis.

Acknowledgements—The author would like to thank Professors R. F. Sekerka and J. S. Langer for their advice and encouragement. The financial support of the Center for the Joining of Materials, NSF Grant Number GH-38399 is also gratefully acknowledged.

† We should indicate that below the incoherent spinodal the alloy is metastable so that incoherent nucleation on the boundary is a possibility in a real alloy. Such a possibility is not encompassed by the present model.

REFERENCES

1. K. Lücke and K. Detert, *Acta Met.* **5,** 628 (1957).
2. J. W. Cahn, *Acta Met.* **10,** 789 (1962).
3. K. Lücke and H. P. Stüwe, *Recovery and Recrystallization of Metals* (edited by L. Himmel), p.171. Interscience, New York (1963).
4. K. Lücke and H. P. Stüwe, *Acta Met.* **19,** 1087 (1971).
5. H. Gleiter, *Phys. Status Solidi* (B) **45,** 9 (1971).
6. F. Larche and J. W. Cahn, *Acta Met.* **21,** 1051 (1973).
7. J. W. Cahn and J. E. Hilliard, *J. chem. Phys.* **28,** 258 (1958).
8. J. W. Cahn, *Acta Met.* **9,** 795 (1961); **10,** 179 (1962).
9. J. E. Hilliard, in *Phase Transformations*, p. 497. A.S.M., Metals Park, Cleveland (1970).
10. M. Hillert, Monograph and Report Series No. 33, p. 231. Institute of Metals, London (1969).
11. M. J. Weins, H. Gleiter and B. Chalmers, *J. appl. Phys.* **42,** 2639 (1971).
12. J. P. Hirth and J. Lothe, *Theory of Dislocations*, p. 669. McGraw-Hill, New York (1968).
13. J. S. Langer and R. F. Sekerka, *Acta Met.* **23,** 1225 (1975).